

Motor Neuron Regeneration in Adult Zebrafish

Michell M. Reimer,¹ Inga Sörensen,² Veronika Kuscha,¹ Rebecca E. Frank,¹ Chong Liu,¹ Catherina G. Becker,^{1*} and Thomas Becker^{1*}

¹Centre for Neuroscience Research, Royal (Dick) School of Veterinary Studies, University of Edinburgh, Summerhall, Edinburgh EH9 1QH, United Kingdom, and ²Medizinische Hochschule Hannover, Molekularbiologie, 30625 Hannover, Germany

The mammalian spinal cord does not regenerate motor neurons that are lost as a result of injury or disease. Here we demonstrate that adult zebrafish, which show functional spinal cord regeneration, are capable of motor neuron regeneration. After a spinal lesion, the ventricular zone shows a widespread increase in proliferation, including slowly proliferating olig2-positive (olig2⁺) ependymo-radial glial progenitor cells. Lineage tracing in olig2:green fluorescent protein transgenic fish indicates that these cells switch from a gliogenic phenotype to motor neuron production. Numbers of undifferentiated small HB9⁺ and islet-1⁺ motor neurons, which are double labeled with the proliferation marker 5-bromo-2-deoxyuridine (BrdU), are transiently strongly increased in the lesioned spinal cord. Large differentiated motor neurons, which are lost after a lesion, reappear at 6–8 weeks after lesion, and we detected ChAT⁺/BrdU⁺ motor neurons that were covered by contacts immunopositive for the synaptic marker SV2. These observations suggest that, after a lesion, plasticity of olig2⁺ progenitor cells may allow them to generate motor neurons, some of which exhibit markers for terminal differentiation and integration into the existing adult spinal circuitry.

Key words: endogenous stem cells; radial glia; BrdU; PCNA; SV2; adult neurogenesis

Introduction

Damage to the spinal cord by injury or motor neuron diseases is devastating because lost neurons are not replaced in the adult mammalian spinal cord (Pinto and Götz, 2007; Bareyre, 2008). Adult zebrafish have an impressively high regenerative capacity, including heart (Poss et al., 2002), retina (Fausett and Goldman, 2006; Bernardos et al., 2007; Fimbel et al., 2007), and functional spinal cord regeneration (Becker et al., 2004). Hence, we asked whether they might be able to regenerate spinal motor neurons, because this might help to elucidate the signals relevant for adult CNS regeneration.

There is significant neurogenesis in specific neurogenic zones even in the unlesioned brain of adult zebrafish (Zupanc et al., 2005; Adolf et al., 2006; Chapouton et al., 2006; Grandel et al., 2006). This is similar to mammals, which probably have fewer of these zones (Gould, 2007). However, the unlesioned adult zebrafish spinal cord shows very little, if any, proliferation and neurogenesis (Zupanc et al., 2005; Park et al., 2007). Therefore, a prerequisite for motor neuron regeneration would be plasticity of relatively quiescent spinal progenitor cells after injury.

These observations prompted us to investigate lesion-induced

neuronal regeneration in the heavily myelinated spinal cord of the fully adult zebrafish (>4 months) after complete spinal transection. We focused on motor neurons because this cell type is often lost as a result of injury or neurodegenerative disease in mammals, and differentiation of motor neurons is highly conserved between mammals and zebrafish. For example, HB9 and islet-1/2 are transcription factors found in developing motor neurons of both mammals (Tsuchida et al., 1994; William et al., 2003) and zebrafish (Cheesman et al., 2004; Park et al., 2004).

We find that substantial numbers of new motor neurons are generated after a spinal lesion, some of which show evidence for terminal differentiation and integration into the spinal circuitry. Lineage tracing identifies olig2-positive (olig2⁺) ependymo-radial glial cells as likely progenitor cells for motor neurons in the lesioned adult spinal cord.

Materials and Methods

Animals. Fish are kept and bred in our laboratory fish facility according to standard methods (Westerfield, 1989), and experiments have been approved by the British Home Office. We used wild-type (wik), HB9:green fluorescent protein (GFP) (Flanagan-Steet et al., 2005), islet-1:GFP (Higashijima et al., 2000), and olig2:GFP (Shin et al., 2003) transgenic fish. Consistency of transgene expression with that of the endogenous genes at the adult stage was verified by immunohistochemistry (HB9: data not shown; islet-1: supplemental Fig. 2, available at www.jneurosci.org as supplemental material) or *in situ* hybridization (olig2; data not shown) for the respective genes.

Spinal cord lesion. As described previously (Becker et al., 2004), fish were anesthetized by immersion in 0.033% aminobenzoic acid ethylester (MS222; Sigma) in PBS for 5 min. A longitudinal incision was made at the side of the fish, and the spinal cord was completely transected under visual control 4 mm caudal to the brainstem–spinal-cord junction.

Electron microscopy. Ultrathin sections (75–100 nm in thickness) were

Received March 19, 2008; revised June 18, 2008; accepted July 11, 2008.

This work was supported by the Deutsche Forschungsgemeinschaft and The Euan MacDonald Centre for Motor Neurone Disease Research. Some of this work is part of the diploma thesis of I.S., performed at the Zentrum für Molekulare Neurobiologie, Hamburg. We thank Drs. B. Appel, D. Meyer, H. Okamoto, and J. Scholes for transgenic fish and reagents, Drs. P. Brophy, S. Lowell, and T. Theil for critically reading this manuscript, and Dr. T. Gillespie for expert advice on confocal microscopy.

*C.G.B. and T.B. contributed equally to this work.

Correspondence should be addressed to Thomas Becker, Centre for Neuroscience Research, Royal (Dick) School of Veterinary Studies, University of Edinburgh, Summerhall, Edinburgh EH9 1QH, UK. E-mail: thomas.becker@ed.ac.uk.
DOI:10.1523/JNEUROSCI.1189-08.2008

Copyright © 2008 Society for Neuroscience 0270-6474/08/288510-07\$15.00/0

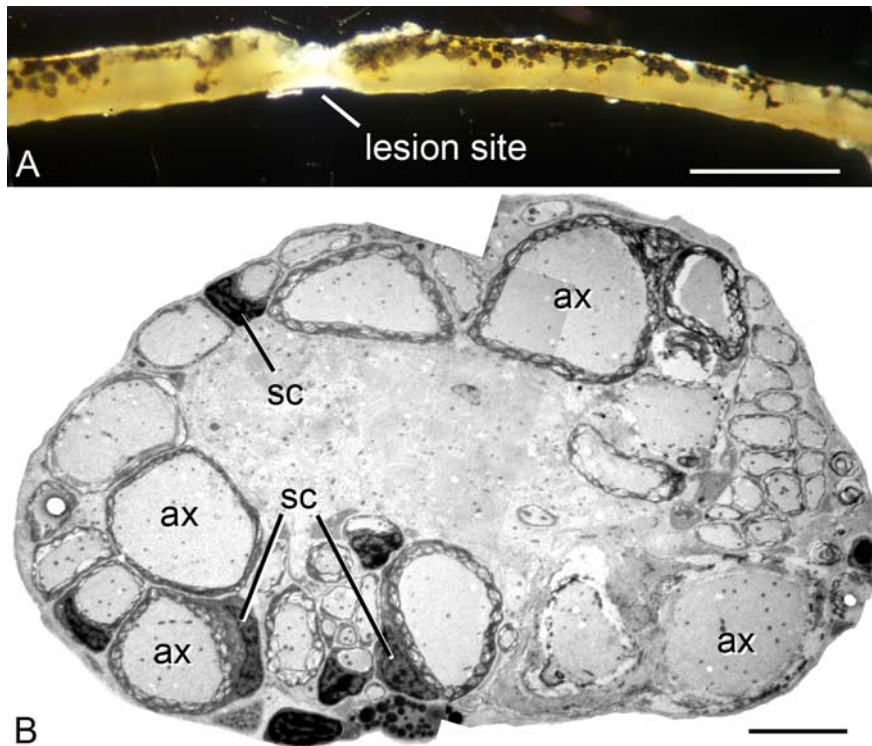


Figure 1. The regenerated spinal cord. *A*, A lateral stereomicroscopic view of a dissected spinal cord is shown (rostral is left). The tissue bridging the lesion site appears translucent. *B*, An electron-microscopic cross section through the lesion site is shown. The lesion site consists mainly of axons (ax), some of which are remyelinated by Schwann cells (sc). Scale bars: *A*, 1 mm; *B*, 5 μ m.

prepared and observed by electron microscopy as published previously (Becker et al., 2004).

Immunohistochemistry. We used rat anti-5-bromo-2-deoxyuridine (BrdU) (BU 1/75, 1:500; AbD Serotec), mouse anti-islet-1/2 (Tsuchida et al., 1994) (40.2D6, 1:1000; Developmental Studies Hybridoma Bank), mouse anti-HB9 (MNR2, 1:400; Developmental Studies Hybridoma Bank), mouse anti-proliferating cell nuclear antigen (PCNA) (PC10, 1:500; DakoCytomation), and goat anti-ChAT (AB144P, 1:250; Millipore Bioscience Research Reagents) antibodies. Secondary cyanine 3 (Cy3)-conjugated antibodies were purchased from Jackson ImmunoResearch. Immunohistochemistry on paraformaldehyde-fixed spinal cord sections (50 μ m thickness) has been described previously (Becker et al., 2004). Antigen retrieval was performed by incubating the sections for 1 h in 2 M HCl for BrdU immunohistochemistry or by incubation in citrate buffer (10 mM sodium citrate in PBS, pH 6.0) at 85°C for 30 min for HB9, islet-1/2, and PCNA immunohistochemistry. Double labeling of cells was always determined in individual confocal sections.

Intraperitoneal BrdU application. Animals were anesthetized and intraperitoneally injected with BrdU (Sigma-Aldrich) solution (2.5 mg/ml) at a volume of 50 μ l at 0, 2, and 4 d after lesion unless indicated otherwise.

Retrograde axonal tracing. Motor neurons in the spinal cord were retrogradely traced by bilateral application of biocytin to the muscle periphery at the level of the spinal lesion, as described previously (Becker et al., 2005), with the modification that biocytin was detected with Cy3-coupled streptavidin (Invitrogen) in spinal sections. This was followed by immunohistochemistry for BrdU (see above).

Cell counts and statistical analysis. Stereological counts were performed in confocal image stacks of three randomly selected vibratome sections from the region up to 750 μ m rostral to the lesion site and three sections from the region up to 750 μ m caudal to the lesion site. Cell numbers were then calculated for the entire 1.5 mm surrounding the lesion site.

PCNA⁺ and BrdU⁺ nuclear profiles in the parenchyma and the ventricular zone (up to one cell diameter away from the ventricular surface) were counted in the same region of spinal cord. At least six sections were analyzed per animal by fluorescence microscopy, and values were ex-

pressed as profiles per section. The observer was blinded to experimental treatments. Variability of values is given as SEM. Statistical significance was determined using the Mann–Whitney *U* test ($p < 0.05$) or ANOVA with Bonferroni's/Dunn's *post hoc* test for multiple comparisons.

Results

A spinal lesion induces widespread ventricular proliferation

To determine the spinal region in which new motor neurons might regenerate, we analyzed the overall organization of the regenerated spinal cord. At 6 weeks after lesion, when functional recovery is complete (Becker et al., 2004), the lesion site itself had not restored normal spinal architecture and consisted mainly of unmyelinated and remyelinated regenerated axons (Fig. 1). Immediately adjacent to this axonal bridge, spinal cross sections showed normal cytoarchitecture, with the exception that white matter tracts were filled with myelin debris of degenerating fibers (Becker and Becker, 2001). This indicated that this tissue existed before the lesion was made. Thus, no significant regeneration of whole spinal cord tissue occurred for up to at least 6 weeks after lesion.

To find newly generated cells in the spinal cord, we used immunohistochemical detection of repeatedly injected BrdU,

which labels cells that have divided. This revealed that very few cells proliferated in the unlesioned spinal cord. At 2 weeks after lesion, the number of newly generated cells in the spinal tissue up to 3.6 mm rostral and caudal to the lesion site increased significantly, covering more than one-third of the length of the entire spinal cord. BrdU⁺ cells were found throughout spinal cross sections but appeared to be concentrated at the midline and in the ventricular zone around the central canal (Fig. 2*A*). Numbers were highest close to the lesion site (Fig. 2*B*).

To localize acutely proliferating cells in the spinal cord, we used immunohistochemistry with the PCNA antibody, which labels cells in early G₁ phase and S phase of the cell cycle. This revealed a significant increase in cell proliferation solely in the ventricular zone. Proliferation peaked at 2 weeks after lesion and returned to values that were similar to those of unlesioned animals by 6 weeks after lesion (Fig. 2*C,D*).

Numbers of differentiating motor neurons increased dramatically in the lesioned spinal cord

We determined whether new motor neurons are generated in the core region of proliferation comprising 1.5 mm surrounding the lesion site. We examined the numbers of cells expressing GFP in transgenic lines, in which GFP expression labels motor neurons under the control of the promoters for HB9 (Flanagan-Steet et al., 2005) or islet-1 (Higashijima et al., 2000). In unlesioned HB9:GFP animals, few large (diameter >12 μ m) motor neurons and very few smaller (diameter <12 μ m) GFP⁺ motor neurons (20 ± 7.7 cells; $n = 4$) were observed in the ventral horn. The number of small HB9:GFP⁺ cells was nonsignificantly increased at 1 week after lesion (207 ± 84.5 cells; $n = 3$; $p = 0.3$) but was significantly increased at 2 weeks after lesion (870 ± 106.8 cells; $n = 11$; $p = 0.004$) (Fig. 3*A*). Similar observations were made in islet-1:GFP

animals (Table 1) (supplemental Fig. 1, available at www.jneurosci.org as supplemental material). Values for HB9:GFP⁺ small motor neurons were reduced again by 6–8 weeks after lesion (251 ± 78.7 cells; $n = 6$). Although still elevated, these values were not significantly different from those in unlesioned animals ($p = 0.2$) (Table 1). Immunohistochemistry for HB9 (data not shown) and *islet-1/2* (supplemental Fig. 2, available at www.jneurosci.org as supplemental material) proteins confirmed the time course of motor neuron numbers and indicated that increases in motor neuron numbers were strongest in the vicinity of the lesion site. Thus, numbers of differentiating motor neurons significantly increased after a spinal lesion.

Double labeling of *islet-1/2* antibodies in HB9:GFP and *islet-1:GFP* transgenic animals revealed that motor neurons were heterogeneous in marker expression (supplemental Fig. 2, available at www.jneurosci.org as supplemental material). This suggests that, similar to development (Tsuchida et al., 1994; William et al., 2003), *islet-1/2* and HB9 expression diverged in spinal motor neurons depending on differentiation stage and/or subtype of motor neuron.

To directly show that new motor neurons were generated after a lesion, we injected animals with BrdU. In lesioned HB9:GFP animals, 200 ± 46.2 cells ($n = 7$; $p = 0.0076$) and in *islet-1:GFP* animals, 184 ± 49.3 cells ($n = 3$; $p = 0.0104$) were double labeled by the transgene and BrdU at 2 weeks after lesion (Fig. 3A) (supplemental Fig. 1, available at www.jneurosci.org as supplemental material). Less than 8% of all BrdU⁺ cells were HB9:GFP⁺ ($7.6 \pm 1.86\%$) or *islet-1:GFP*⁺ ($6.3 \pm 1.75\%$), suggesting proliferation of additional neuronal and non-neuronal cell types. Thus, a spinal lesion induces generation of new motor neurons and possibly other cell types in adult zebrafish.

In contrast, in the unlesioned spinal cord, we observed no double-labeled motor neurons in *islet-1:GFP* animals ($n = 5$) and only one cell so labeled in HB9:GFP animals ($n = 4$). Even an extended BrdU injection protocol (injections at days 0, 2, 4, 6, and 8, analysis at day 14) did not yield any HB9:GFP⁺/BrdU⁺ cells in unlesioned fish ($n = 5$). Because the bioavailability of BrdU is ~4 h after injection (Zupanc and Horschke, 1995), we cannot exclude a very low proliferation rate of motor neurons. However, we do not find evidence for substantial motor neuron generation in the unlesioned mature spinal cord.

New motor neurons are likely derived from olig2-expressing ependymo-radial glial cells

Olig2 is essential for motor neuron generation during development (Park et al., 2004). In adult olig2:GFP transgenic fish, GFP is

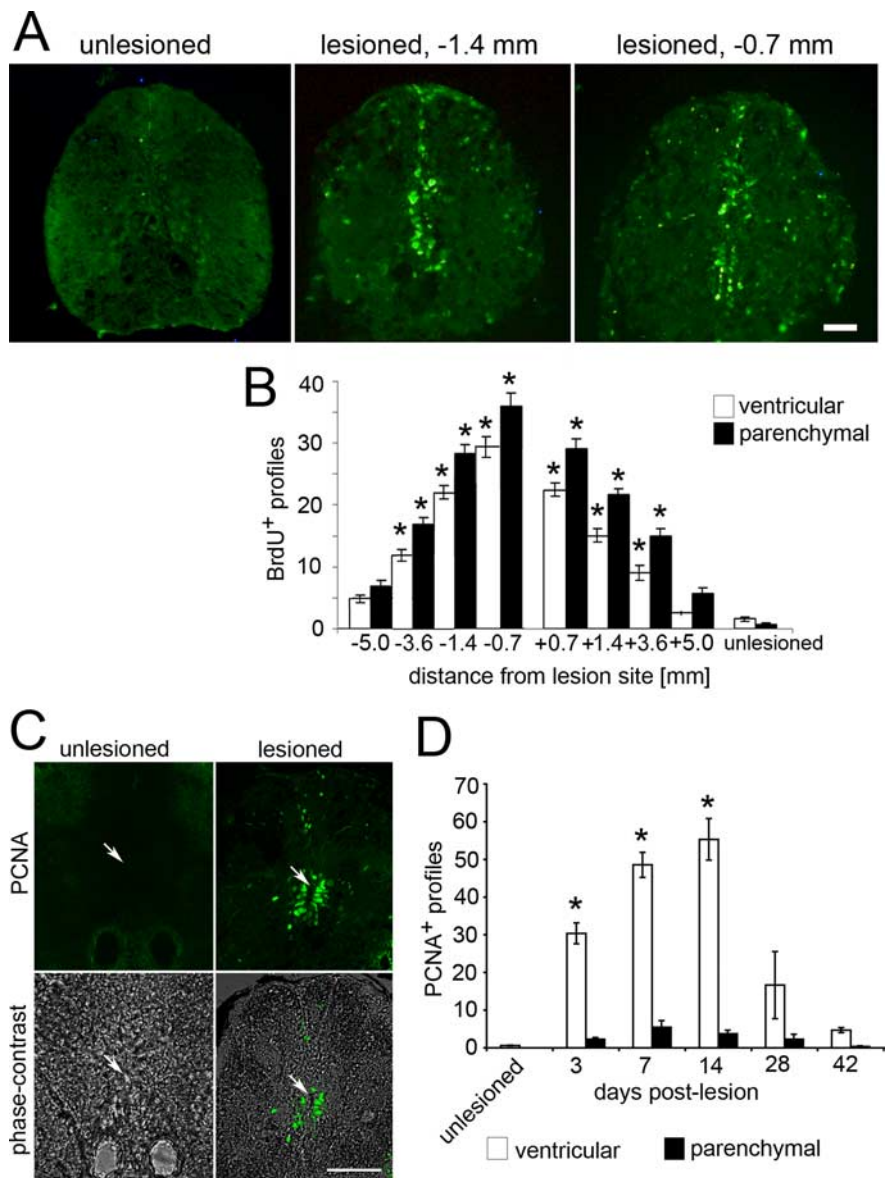


Figure 2. Lesion-induced proliferation in the adult spinal cord. Confocal images of spinal cross sections are shown (dorsal up). **A**, BrdU labeling is massively increased at 14 d after lesion. The highest density of BrdU⁺ cells is detectable in the ventricular zone close to the lesion site. **B**, Numbers of BrdU⁺ profiles are significantly increased up to 3.6 mm rostral and caudal to the lesion epicenter ($n = 3$ animals per treatment; $p < 0.0001$) at 2 weeks after lesion. Although the nonventricular area of spinal cross sections is much larger than that of the ventricular zone, only slightly more proliferating cells were observed in the nonventricular area, indicating a high density of labeled cells in the ventricular zone. **C**, PCNA immunohistochemistry indicates a strong increase in the number of proliferating cells in the ventricular zone (arrows) at 14 d after lesion. **D**, The number of proliferating ventricular, but not parenchymal, cell profiles per section was significantly increased after a lesion ($n = 3$ animals per time point; $p < 0.0001$). * indicates significantly different from unlesioned controls. Scale bars: **A**, 25 μm ; **C**, 50 μm .

found in oligodendrocytes and in a ventrolateral subset of ependymo-radial glial cells (Fig. 3B) (Park et al., 2007). After a lesion, these cells proliferated, as indicated by substantial double labeling with PCNA at 2 weeks after lesion (490 ± 224.2 PCNA⁺/olig2:GFP⁺ ependymo-radial glial cells and 217 ± 103.8 non-ventricular PCNA⁺/olig2:GFP⁺ cells; $n = 2$). Thus, olig2-expressing cells could give rise to motor neurons during regeneration.

To analyze the relationship between olig2-expressing potential stem cells and motor neurons more directly, we used immunohistochemistry for HB9 and *islet-1/2* in olig2:GFP transgenic animals. The relative stability of GFP has been used as a lineage

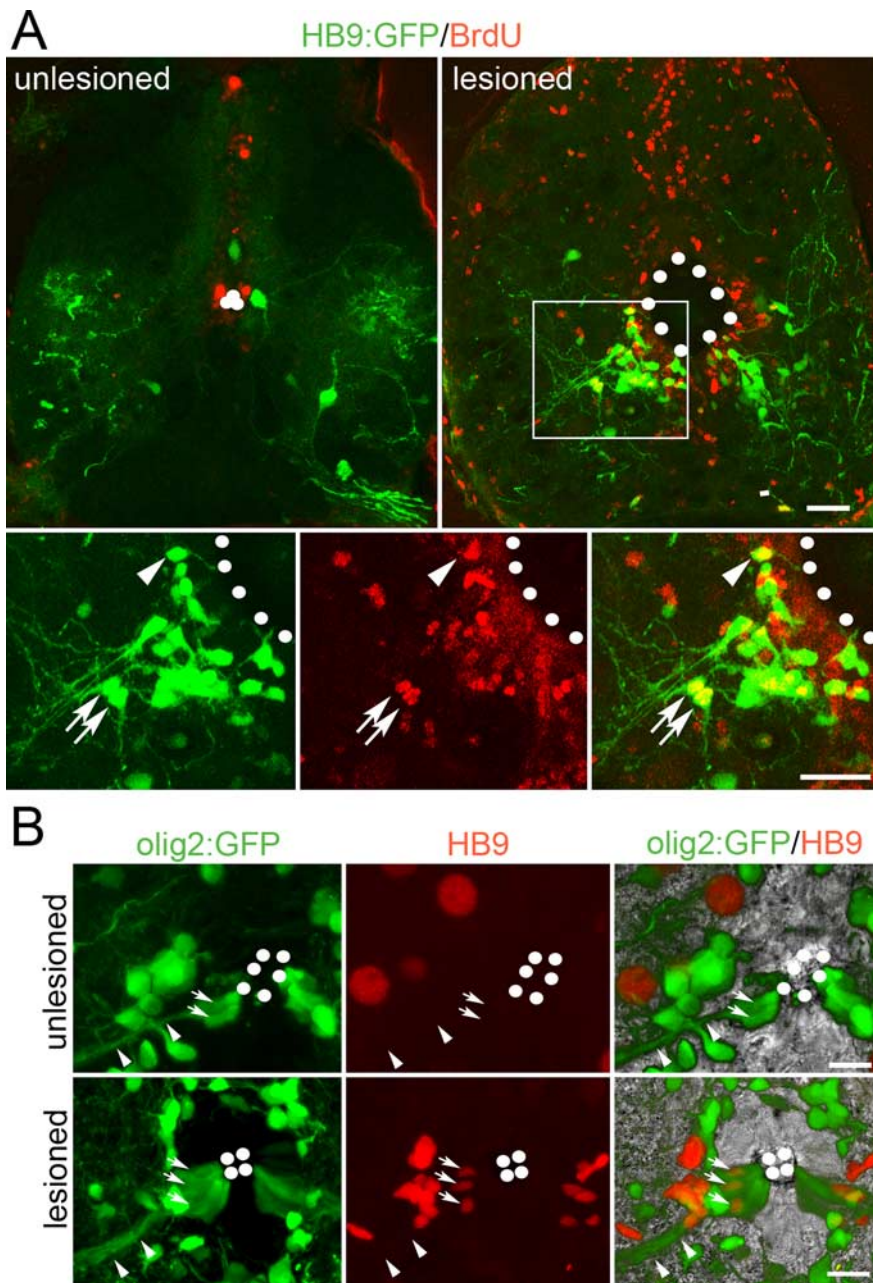


Figure 3. Generation of new motor neurons in the lesioned spinal cord. Confocal images of spinal cross sections at 2 weeks after lesion are shown (dorsal is up; dots outline the ventricle). **A**, HB9:GFP⁺/BrdU⁺ neurons are present in the lesioned, but not the unlesioned, ventral horn. These cells (boxed in top right and shown at higher magnification in bottom row) bear elaborate processes (arrows) or show ventricular contact (arrowhead). **B**, olig2:GFP⁺ progenitor cells (arrows) have long radial processes (arrowheads), contact the ventricle, and are HB9⁺ in the lesioned, but not the unlesioned, spinal cord. Scale bars: **A**, 25 μ m; **B**, top row, 7.5 μ m; **B**, bottom row, 15 μ m.

tracer in transgenic fish to determine the progeny of adult retinal (Bernardos et al., 2007) and tegmental (Chapouton et al., 2006) progenitor cells. In unlesioned animals, no double labeling of GFP and HB9 ($n = 3$) or GFP and islet-1/2 ($n = 4$) was observed. At 2 weeks after lesion, single parenchymal olig2:GFP⁺ cells did not coexpress either HB9 or islet-1/2, which makes it unlikely that these cells gave rise to motor neurons. In contrast, a substantial subpopulation of olig2:GFP⁺ ependymo-radial glial cells were HB9⁺ (204 ± 32.2 cells; $n = 3$) (Fig. 3B) or islet-1/2⁺ (34 ± 8.9 cells; $n = 4$; data not shown). Double labeling indicated that either there was an overlap in the expression of olig2 and HB9 or

islet-1/2 during differentiation of motor neurons in the ventricular zone or recently differentiated HB9⁺ and islet-1/2⁺ motor neurons had retained the GFP. Differences in the numbers of olig2:GFP⁺ ependymo-radial glial cells that coexpressed HB9 or islet-1/2 may be related to differences in differentiation stage or subtype of motor neuron produced (William et al., 2003). To demonstrate that HB9⁺/olig2:GFP⁺ cells are newly generated, we used HB9, olig2:GFP, and BrdU triple labeling. Indeed, 74 ± 22.7 HB9⁺/olig2:GFP⁺/BrdU⁺ cells ($n = 3$) were found exclusively in the zone continuous with olig2:GFP⁺ cells at the ventricle at 14 d after lesion (supplemental Fig. 3, available at www.jneurosci.org as supplemental material). In the ventricular zone dorsal and ventral to the olig2:GFP⁺ region, expression of HB9 or islet-1/2 was rarely observed, suggesting that olig2:GFP⁺ ependymo-radial glial cells were the main source of new motor neurons (Fig. 3B). Thus, olig2 expressing ependymo-radial glial cells proliferate and switch to motor neuron production after a lesion.

To determine whether olig2:GFP⁺ ependymo-radial glial cells had stem cell characteristics, we determined whether they retained BrdU label and were thus slowly proliferating (Chapouton et al., 2006). Lesioned olig2:GFP animals were injected with a single pulse of BrdU at 14 d after lesion, and the number of olig2:GFP⁺/BrdU⁺ cells in the ventricular zone was assessed at 4 h and 14 d after injection. Numbers were not significantly different at the two time points (4 h, 60 ± 11.5 cells, $n = 5$; 14 d, 53 ± 13.3 cells, $n = 4$; $p = 0.6$), indicating that olig2:GFP⁺ cells did indeed retain label (supplemental Fig. 4, available at www.jneurosci.org as supplemental material). This suggests the possible presence of motor neuron stem cells among the population of olig2:GFP⁺ ependymo-radial glial cells. However, we cannot exclude that label-retaining olig2:GFP⁺ cells also give rise to other cell types.

Evidence for terminal differentiation of new motor neurons

Newly generated small motor neurons were not fully differentiated at 2 weeks after lesion. They were either attached to the ventricle with a single slender process or were located farther away from the ventricle with several processes, some of which exceeded 100 μ m in length, extending into the gray matter in HB9:GFP and in islet-1:GFP transgenic fish (Figs. 3A, 4). However, even the cells with long processes showed very little apposition of somata and processes with SV2⁺ contacts, an indicator of synaptic coverage (Fig. 4B). Moreover, small HB9:GFP⁺ neurons rarely expressed ChAT ($2.7 \pm 0.90\%$; $n = 3$), a marker of

Table 1. Dynamics of motor neuron numbers after spinal cord lesion

	HB9:GFP		Islet-1:GFP		ChAT
	Large cells	Small cells	Large cells	Small cells	Large cells
Unlesioned	133 ± 34.9	20 ± 7.7 (<i>n</i> = 4)	78 ± 17.2	27 ± 3.9 (<i>n</i> = 5)	478 ± 111.1 (<i>n</i> = 3)
1 week	42 ± 15.1*	207 ± 84.5 (<i>n</i> = 3)	n.d.	n.d.	n.d.
2 weeks	40 ± 7.3*	870 ± 106.8 (<i>n</i> = 11)*	32 ± 9.5	870 ± 244.9 (<i>n</i> = 4)	235 ± 40.9 (<i>n</i> = 3)
6–8 weeks	91 ± 11.5	251 ± 78.7 (<i>n</i> = 6)	n.d.	n.d.	348 ± 67.3 (<i>n</i> = 4)

**p* < 0.05, significantly different from unlesioned control. n.d., Not determined.

mature motor neurons (Arvidsson et al., 1997), at 2 weeks after lesion (Fig. 4A).

In contrast to small HB9:GFP⁺ cells, large HB9:GFP⁺ cells were mostly ChAT⁺ in unlesioned animals (80.6 ± 7.99%; *n* = 3), indicating that these were fully differentiated motor neurons. At 1 (42 ± 15.1 cells; *n* = 3; *p* = 0.0035) and 2 (40 ± 7.3 cells; *n* = 11; *p* < 0.0003) weeks after lesion, large-diameter HB9:GFP⁺ motor neurons were strongly reduced in number compared with unlesioned animals (133 ± 34.9 cells; *n* = 4). This suggests lesion-induced loss of motor neurons, which was confirmed by terminal deoxynucleotidyl transferase-mediated biotinylated UTP nick end labeling of 22.8 ± 11.39% of the HB9:GFP⁺ motor neurons at 3 d after lesion (*n* = 3) (supplemental Fig. 5, available at www.jneurosci.org as supplemental material).

At 6–8 weeks after lesion, there was an increase in the number of large-diameter HB9:GFP⁺ cells to 91 ± 11.5 cells (*n* = 6), such that cell numbers were not different from those in unlesioned animals (*p* = 0.081). Large-diameter islet-1:GFP⁺ and ChAT⁺ cells showed similar dynamics (Table 1). This suggests that some newly generated motor neurons matured and replaced lost motor neurons. Other newly generated cells might have died, as indicated by increased association with macrophages/microglial cells between 2 and 6 weeks after lesion (supplemental Fig. 6, available at www.jneurosci.org as supplemental material).

To directly demonstrate the presence of newly generated, terminally differentiated motor neurons, we used triple labeling of BrdU, ChAT, and SV2 at 6 weeks after lesion. In the 1500 μm surrounding the lesion site, we found 29 ± 23.1 large BrdU⁺/ChAT⁺ cells (*n* = 3) covered with SV2⁺ contacts at a density that was comparable with that of motor neurons in unlesioned animals (Fig. 4C). Application of the axonal tracer biocytin to the muscle periphery labeled one BrdU⁺ cell in a motor neuron position in the ventromedial spinal cord near the lesion site (*n* = 8; 6–14 weeks after lesion) (Fig. 4D). This suggests that some newly generated motor neurons were integrated into the spinal circuitry and grew an axon out of the spinal cord.

Discussion

We show here for the first time that a spinal lesion triggers generation of motor neurons in the spinal cord of adult zebrafish. Lesion-induced proliferation and motor neuron marker expression in olig2⁺ ependymo-radial glial cells makes these the likely motor neuron progenitor cells. Some of the newly generated motor neurons show markers for terminal differentiation and network integration.

Newly generated motor neurons are added to preexisting spinal tissue adjacent to a spinal lesion site in which normal cytoarchitecture is not restored. Thus, this model differs significantly from tail regeneration paradigms in amphibians in which the entire spinal cord tissue is completely reconstructed from an advancing blastema (Echeverri and Tanaka, 2002).

Our results suggest olig2⁺ ependymo-radial glial cells to be the progenitor cells for spinal motor neurons, because a lesion

induces their proliferation and lineage tracing indicated that a substantial number of newly generated olig2:GFP⁺ ependymo-radial glial cells coexpressed the motor neuron markers HB9 or islet-1/2. Moreover, parenchymal olig2:GFP⁺ cells were never, and ependymo-radial glial cells outside the olig2:GFP⁺ zone were rarely, labeled by HB9 or islet-1/2 antibodies. This supports the hypothesis that olig2:GFP⁺ ependymo-radial glial cells are the main source of motor neurons after a lesion. However, we cannot exclude the possibility that some motor neurons might have regenerated from as yet unidentified olig2-negative (olig2⁻) parenchymal progenitors.

During postembryonic development, olig2:GFP⁺ cells only give rise to oligodendrocytes (Park et al., 2007). Thus, adult neuronal regeneration is not just a continuation of a late developmental process but an indication of significant plasticity of adult spinal progenitor cells in the fully mature spinal cord.

Additionally, olig2⁺ ependymo-radial glial cells have characteristics of neural stem cells. They are label retaining, and lesion-induced proliferation of these cells leads only to a moderate increase in their number, suggesting asymmetric cell divisions and some potential for self-renewal. Moreover, these cells express brain lipid binding protein, which is also expressed in mammalian radial glial stem cells, and the PAR (partitioning-defective) complex protein atypical PKC, an indicator of asymmetric cell division, at postembryonic stages (Park et al., 2007). A stem cell role for olig2⁺ ependymo-radial glial cells would be in agreement with that of other radial glia cell types in developing mammals and in adult zebrafish (Pinto and Götz, 2007). For example, Müller cells, the radial glia cell type in the adult retina, can produce different cell types in adult zebrafish depending on which cells are lost after specific lesions (Fausett and Goldman, 2006; Bernardos et al., 2007; Fimbel et al., 2007).

We observed that numbers of differentiated motor neurons, i.e., large HB9:GFP⁺ cells and ChAT⁺ cells, were reduced at 2 weeks after lesion and recovered at 6–8 weeks after lesion. This suggests that motor neurons regenerate and is in agreement with previous observations in the guppy (*Poecilia reticulata*), in which large “ganglion cells” disappeared and reappeared after a lesion (Kirsche, 1950). In accordance with this finding, we detected terminally differentiated (ChAT⁺), newly generated (BrdU⁺) motor neurons that were covered by SV2⁺ contacts at 6–8 weeks after lesion, suggesting their integration into the spinal network. The rare observation of one BrdU⁺ cell that was traced from the muscle periphery indicates that newly generated motor neurons may even be capable of growing their axons out of the spinal cord toward muscle targets. In contrast, at early time points, a transient population of small, newly generated motor neurons (HB9:GFP⁺, islet-1:GFP⁺) that were not fully differentiated (ChAT⁻) and not decorated by SV2⁺ contacts were present in large numbers. These cells varied in motor neuron marker expression and the extent of process elaboration. Together, these observations suggest that motor neurons are generated and undergo successive

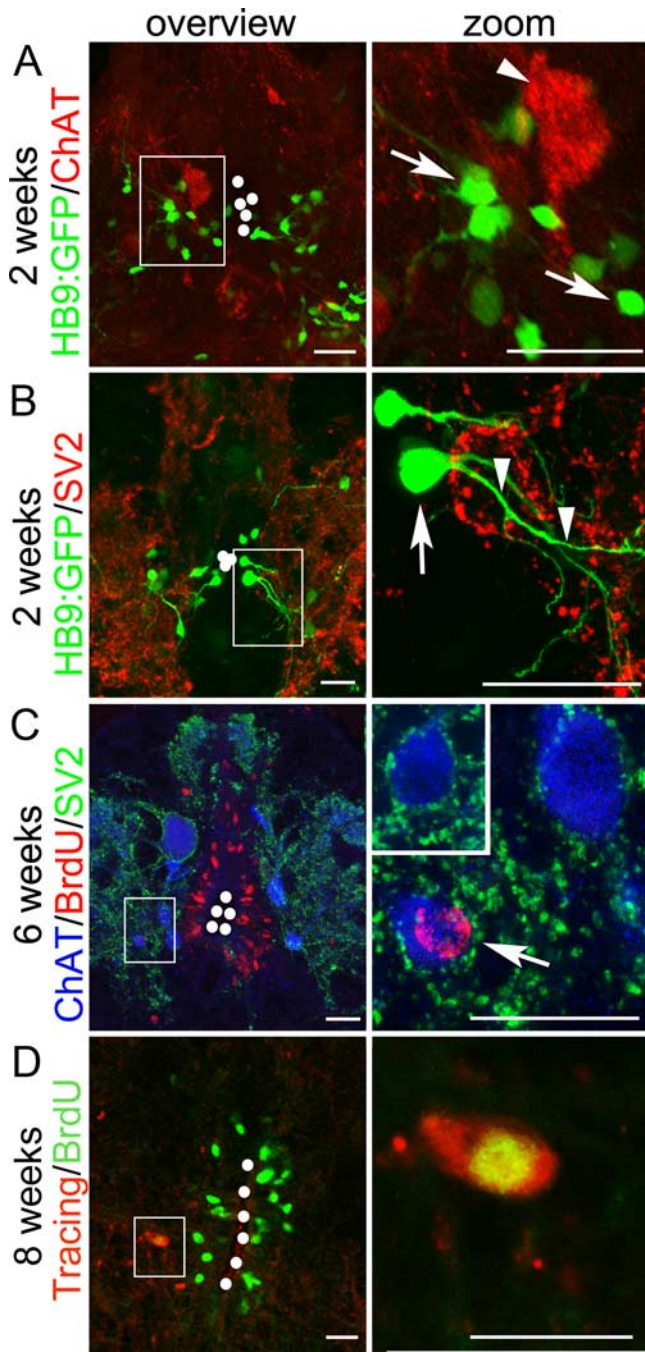


Figure 4. Maturation of newly generated motor neurons. Confocal images of spinal cross sections are shown (dorsal is up, dots outline the ventricle). **A**, Newly generated HB9:GFP⁺ motor neurons are ChAT⁻ (arrows; arrowhead indicates a ChAT⁺/HB9:GFP⁻ differentiated motor neuron). **B**, Somata (arrow) and proximal dendrites (arrowheads) receive few SV2⁺ contacts at 2 weeks after lesion. **C**, At 6 weeks after lesion, ChAT⁺/BrdU⁺ somata are decorated with SV2⁺ contacts (arrow). Inset (right) depicts a ChAT⁺ motor neuron decorated with SV2⁺ contacts in an unlesioned animal. **D**, At 8 weeks after lesion, a BrdU⁺ cell is retrogradely traced from the muscle tissue. Scale bars: **A–C**, 25 μ m; **D**, 15 μ m.

morphological and gene expression differentiation steps toward integration into an existing spinal network after a lesion.

A spinal lesion in mammals leads to proliferation and expression of nestin (Shibuya et al., 2002) as well as Pax6 (Yamamoto et al., 2001), which are markers for progenitor cells, around the ventricle. In addition, parenchymal astrocytes, some of which carry radial processes, express nestin. However, olig2 and several

other factors are not re-expressed (Ohori et al., 2006). These observations suggest that spinal progenitors in adult mammals show some plasticity after a lesion and could potentially be induced to produce new motor neurons.

We conclude that the zebrafish, a powerful genetically tractable model, provides an opportunity to identify the evolutionarily conserved signals that trigger massive stem cell-derived regeneration and network integration of motor neurons in the adult spinal cord.

References

- Adolf B, Chapouton P, Lam CS, Topp S, Tannhäuser B, Strähle U, Götz M, Bally-Cuif L (2006) Conserved and acquired features of adult neurogenesis in the zebrafish telencephalon. *Dev Biol* 295:278–293.
- Arvidsson U, Riedl M, Elde R, Meister B (1997) Vesicular acetylcholine transporter (VAcHT) protein: a novel and unique marker for cholinergic neurons in the central and peripheral nervous systems. *J Comp Neurol* 378:454–467.
- Bareyre FM (2008) Neuronal repair and replacement in spinal cord injury. *J Neurol Sci* 265:63–72.
- Becker CG, Lieberoth BC, Morellini F, Feldner J, Becker T, Schachner M (2004) L1.1 is involved in spinal cord regeneration in adult zebrafish. *J Neurosci* 24:7837–7842.
- Becker T, Becker CG (2001) Regenerating descending axons preferentially reroute to the gray matter in the presence of a general macrophage/microglial reaction caudal to a spinal transection in adult zebrafish. *J Comp Neurol* 433:131–147.
- Becker T, Lieberoth BC, Becker CG, Schachner M (2005) Differences in the regenerative response of neuronal cell populations and indications for plasticity in intraspinal neurons after spinal cord transection in adult zebrafish. *Mol Cell Neurosci* 30:265–278.
- Bernardos RL, Barthel LK, Meyers JR, Raymond PA (2007) Late-stage neuronal progenitors in the retina are radial Muller glia that function as retinal stem cells. *J Neurosci* 27:7028–7040.
- Chapouton P, Adolf B, Leucht C, Tannhäuser B, Ryu S, Driever W, Bally-Cuif L (2006) *her5* expression reveals a pool of neural stem cells in the adult zebrafish midbrain. *Development* 133:4293–4303.
- Cheesman SE, Layden MJ, Von Ohlen T, Doe CQ, Eisen JS (2004) Zebrafish and fly Nkx6 proteins have similar CNS expression patterns and regulate motoneuron formation. *Development* 131:5221–5232.
- Echeverri K, Tanaka EM (2002) Ectoderm to mesoderm lineage switching during axolotl tail regeneration. *Science* 298:1993–1996.
- Fausett BV, Goldman D (2006) A role for α 1 tubulin-expressing Muller glia in regeneration of the injured zebrafish retina. *J Neurosci* 26:6303–6313.
- Fimbel SM, Montgomery JE, Burket CT, Hyde DR (2007) Regeneration of inner retinal neurons after intravitreal injection of ouabain in zebrafish. *J Neurosci* 27:1712–1724.
- Flanagan-Steet H, Fox MA, Meyer D, Sanes JR (2005) Neuromuscular synapses can form in vivo by incorporation of initially aneural postsynaptic specializations. *Development* 132:4471–4481.
- Gould E (2007) How widespread is adult neurogenesis in mammals? *Nat Rev Neurosci* 8:481–488.
- Grandel H, Kaslin J, Ganz J, Wenzel I, Brand M (2006) Neural stem cells and neurogenesis in the adult zebrafish brain: origin, proliferation dynamics, migration and cell fate. *Dev Biol* 295:263–277.
- Higashijima S, Hotta Y, Okamoto H (2000) Visualization of cranial motor neurons in live transgenic zebrafish expressing green fluorescent protein under the control of the islet-1 promoter/enhancer. *J Neurosci* 20:206–218.
- Kirsche W (1950) The regenerative events on the spinal cord of grown up teleosts after operative dissection (in German). *Z Mikrosk Anat Forsch* 56:190–263.
- Ohori Y, Yamamoto S, Nagao M, Sugimori M, Yamamoto N, Nakamura K, Nakafuku M (2006) Growth factor treatment and genetic manipulation stimulate neurogenesis and oligodendrogenesis by endogenous neural progenitors in the injured adult spinal cord. *J Neurosci* 26:11948–11960.
- Park HC, Shin J, Appel B (2004) Spatial and temporal regulation of ventral spinal cord precursor specification by Hedgehog signaling. *Development* 131:5959–5969.

- Park HC, Shin J, Roberts RK, Appel B (2007) An olig2 reporter gene marks oligodendrocyte precursors in the postembryonic spinal cord of zebrafish. *Dev Dyn* 236:3402–3407.
- Pinto L, Götz M (2007) Radial glial cell heterogeneity: the source of diverse progeny in the CNS. *Prog Neurobiol* 83:2–23.
- Poss KD, Wilson LG, Keating MT (2002) Heart regeneration in zebrafish. *Science* 298:2188–2190.
- Shibuya S, Miyamoto O, Auer RN, Itano T, Mori S, Norimatsu H (2002) Embryonic intermediate filament, nestin, expression following traumatic spinal cord injury in adult rats. *Neuroscience* 114:905–916.
- Shin J, Park HC, Topczewska JM, Mawdsley DJ, Appel B (2003) Neural cell fate analysis in zebrafish using olig2 BAC transgenics. *Methods Cell Sci* 25:7–14.
- Tsuchida T, Ensini M, Morton SB, Baldassare M, Edlund T, Jessell TM, Pfaff SL (1994) Topographic organization of embryonic motor neurons defined by expression of LIM homeobox genes. *Cell* 79:957–970.
- Westerfield M (1989) *The zebrafish book: a guide for the laboratory use of zebrafish (Brachydanio rerio)*. Eugene, OR: University of Oregon Press.
- William CM, Tanabe Y, Jessell TM (2003) Regulation of motor neuron subtype identity by repressor activity of Mnx class homeodomain proteins. *Development* 130:1523–1536.
- Yamamoto S, Nagao M, Sugimori M, Kosako H, Nakatomi H, Yamamoto N, Takebayashi H, Nabeshima Y, Kitamura T, Weinmaster G, Nakamura K, Nakafuku M (2001) Transcription factor expression and Notch-dependent regulation of neural progenitors in the adult rat spinal cord. *J Neurosci* 21:9814–9823.
- Zupanc GK, Horschke I (1995) Proliferation zones in the brain of adult gymnotiform fish: a quantitative mapping study. *J Comp Neurol* 353:213–233.
- Zupanc GK, Hinsch K, Gage FH (2005) Proliferation, migration, neuronal differentiation, and long-term survival of new cells in the adult zebrafish brain. *J Comp Neurol* 488:290–319.